Journal of Photoscience

LASER ABLATION: FUNDAMENTALS AND APPLICATIONS IN MICROPATTERNING AND THIN FILM FORMATION

J. HEITZ[1], D. BÄUERLE[1], E. ARENHOLZ[1], N. ARNOLD[1] AND J. T. DICKINSON[2]
[1]Johannes-Kepler-Universität Linz, Angewandte Physik, A-4040 Linz, Austria
[2]Washington State University, Pullman, WA 99164-2814, USA

Reprinted from
Journal of Photoscience, Vol. 6, No. 3, pp. 103 – 108

Journal of Photoscience, Vol. 6, No. 3, pp. 103 – 108

LASER ABLATION: FUNDAMENTALS AND APPLICATIONS IN MICROPATTERNING AND THIN FILM FORMATION

J. HEITZ[1], D. BÄUERLE[1], E. ARENHOLZ[1], N. ARNOLD[1] AND J. T. DICKINSON[2]
[1]Johannes-Kepler-Universität Linz, Angewandte Physik, A-4040 Linz, Austria
[2]Washington State University, Pullman, WA 99164-2814, USA

(*Received* 28 *June* 1999; *accepted* 30 *July* 1999)

Abstract –We present recent results on ablation mechanism, single-pulse laser micropatterning, pulsed-laser deposition (PLD) and particulates formation accompanying laser ablation, with special emplasis on polymers, in particular polyimide, (PI), and polytetrafluoroethylene, (PTFE). Ablation of polymers is described on the basis of photothermal bond breaking within the bulk material. Here, we assume a first order chemical reaction, which can be described by an Arrhenius law. Ablation starts when the density of broken bonds at the surface reaches a certain critical value. Single-pulse laser ablation of polyimide shows a clear pulse-length dependence of the threshold fluence. This experimental result strongly supports a thermal ablation model. We discuss the various possibilities and drawbacks of PLD and describe the morphology, physical properties and applications of PTFE films.

INTRODUCTION

Pulsed-laser ablation and deposition have found increasing interest in surface patterning and thin-film fabrication.[1] Especially the UV-laser ablation of polymers has been the subject of a great number of publications and also found many technical applications, although the physical and chemical mechanisms involved are still under discussion.[2] In most experiments, ablation rates are derived from the total ablated depthobtained after multiple-pulse irradiation at different laser fluences and wavelength. Due to incubation effects, however, the data derived from such experiments do not permit a proper analysis of the fundamental interaction mechanisms Therefore, we measured single-pulse ablation rates by using focused UV-Ar^+-laser radiation and atomic force microscopy (AFM).[3]

PLD has become a very popular technique for the fabrication of thin films of multicomponent materials. It is of particular interest because it enables one to fabricate multicomponent stoichiometric films from a single target. among the materials studied in most detail are compound semiconductors, dielectrics, ferroelectrics, electrooptic and giant magnetoresistance oxides, high-temperature superconductors, polymers, and various types of heterostructures. PLD is very reliable, offers great experimental versatility, it is fairly simple and fast-as long as small-area films of up to several square-centimeters are to be fabricated. For these reasons, PLD is particularly suitable in materials research and development. The strong non-equilibrium conditions in PLD allow, however, some unique applications: Among those are metastable materials that cannot be synthesized by standard techniques and the fabrication of films from species that are generated only during pulsed-laser ablation. With certain systems, the physical properties of such films are superior to those fabricated by standard evaporation, electron-beam evaporation, etc. We have produced high-quality PTFE films by means of PLD.[4] These films proved to be excellent long-time charge storage media[5] superior to those produced by

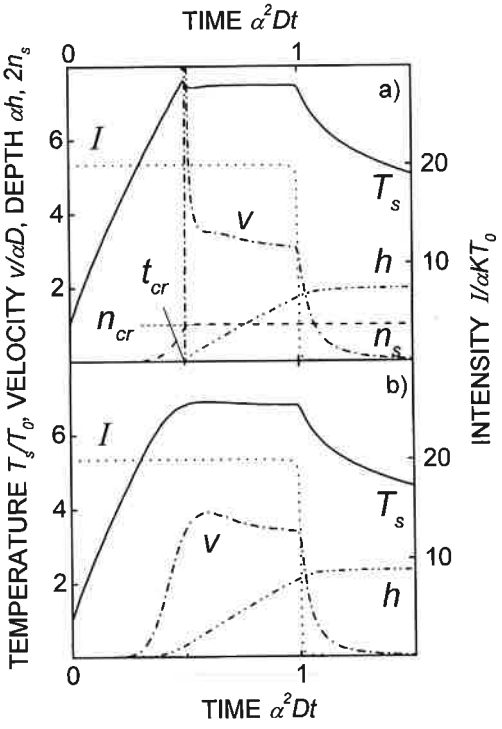

Figure 1. Onset of ablation for volume and surface models with constant intensity(dotted curve). Surface temperature T_s (solid curve), fraction of broken bonds at the surface n_s (dashed curve), recession velocity ν (dash-dot), and ablated depth h (dashdouble dot). (a) Volume model. (b) Surface model.[2]

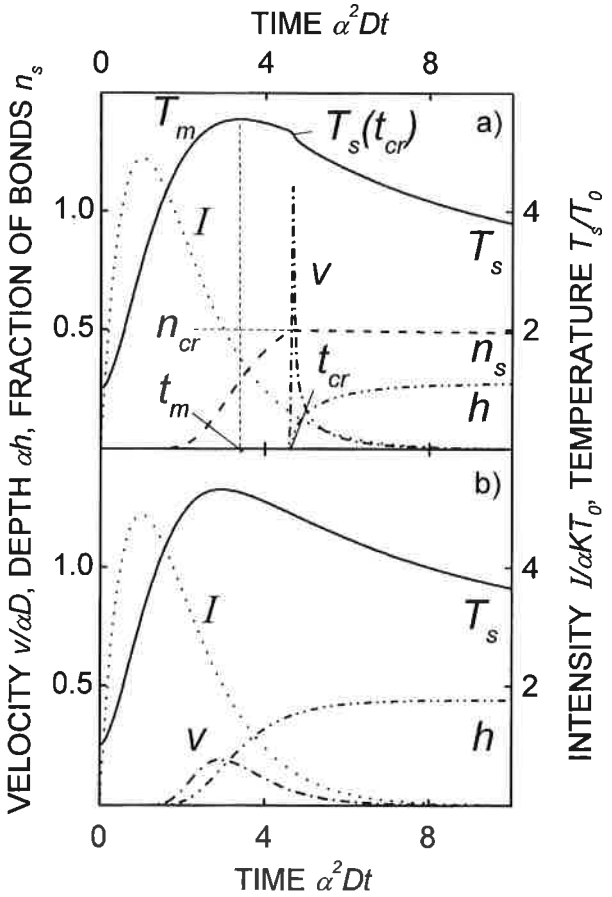

Figure 2. Near threshold ablation with smooth laser pulse for volume and surfae models. Surfact temperature T_s (solid curve), fraction of broken bonds at the surface n_s (dashed curve), recession velocity v (dash-dot), and ablated depth h (dashdouble dot). (a) Volume model. (b) Surface model.[2]

other techniques.

Besides restrictions with respect to film areas, in many cases the major disadvantage of PLD is related to particulates that appear on the substrate and film surface. On the other hand, some applications require the formation of nano- or microparticulates. For instance, considerable effort has been recently focused on generating ultra-fine PTFE particles for coatings in micro-electronics. Particulate ejection mechanisms accompanying pulsed laser ablation can be classified to four main types: Solified liquid droplets, which may be either related to vapor condensate and /or thermodynamical instabilities at the molten traget surface, irregulary shaped solid grains, solidified splash drops and, at least with polymers and biological materials, high molecular weight fragments and clusters. Additional structures may be formed directly at the substrate surfacel. Many of these particulates are not neutral, but are carrying electrical charge, which can influence the film formation and the aggregation of small particulates.[6,7]

Fundamental ablation mechanisms

The primary step in UV-laser ablation is the absorption of the laser light by the electrons. The dissipation of the excitation energy can proceed along different channels. Let us first enumerate experimental facts, which motivate further theoretical considerations. It is well-known that ablation rates are measured by different techniques that yield non-equivalent results, in particular near the threshold fluence for ablation ϕ_{th}:

- The ablated depth measured by profilometry starts sharply at fluence $\phi = \phi_{th}$.
- The ablation rate recalculated from mass loss measurements using a quartz crystal microbalance (QCM)[8] or mass spectrometry reveals an Arrhenius tail.
- Ablation is frequently accompanied by chemical and/or physical modification of material within a certain depth.

Different models were applied for the description of UV-laser ablation of polymers. One can distingusih between photochemical models, where electronic excitations result in direct bond breaking (without thermalization), and models, where the bonds are thermally broken. The thermal nature of the ablation process is supported by the observation of an Arrhenius tail and the dependence of the ablation rate and threshold on the laser pulse lenght (see next paragraph). With photophysical models both thermal and non-thermal mechanisma are important. The latter model apply to ps and fs laser ablation.[9,10]

From another perspective, the present models can be subdivided into volume and surface models. With surface models, the processes responsible for material removal takes place only within several monolayers of the surface. As a result, the velocity of the interface between the gaseous and condensed phase depends explicitly only on the surface temperature or laser-light intensity. With volume models, the processes, which lead to the decomposition of the materials, take place within the bulk. This is in accordance with the observed surface modifications.

Thermal volume models are often oversimplified, they frequently ignore the influence of the moving boundary in the heat equation, which resulted in unrealistically high temperatures. Therefore, we present here a thermal volume nodel, which includes the effects of the moving boundary, and study its implications.

Light absorption shall follow Beer's law:

$$\frac{\partial I}{\partial z} = -\alpha I \tag{1}$$

The electronic excitations thermalize on aps time scale[11]. Heating shall be described by the one-dimensional heat equation. Subsequently, we employ a moving reference frame, which is fixed with the ablation front.

$$\frac{\partial H}{\partial t} = v\frac{\partial H}{\partial z} + \frac{\partial}{\partial z}\left(K\frac{\partial T}{\partial z}\right) - \frac{\partial I}{\partial z} - L(1-n_b)k_0\exp(-T_a/T) \tag{2}$$

Here T is the temperature, K the thermal conductivity,

$$H = \rho\int_{T_0}^{T} c(T')dT' \tag{3}$$

is the volumetric enthaply with c being the specific heat, ρ(con-

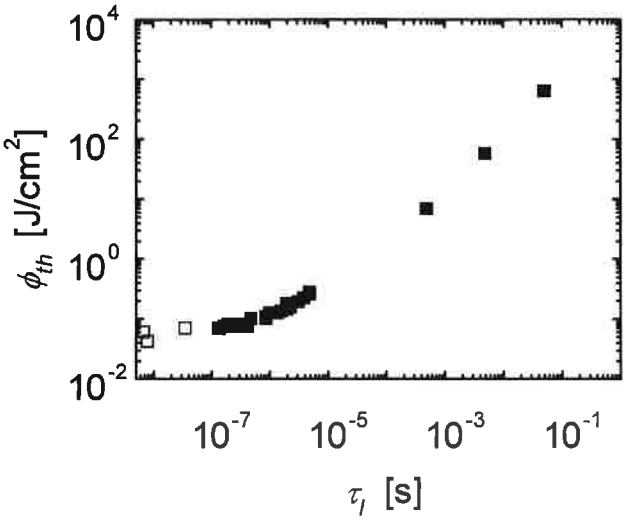

Figure 3. Experimental[8] and theoretical curves[2] for KrF laser ablation of PI. Mass loss *via* volatile species h_M (dashed curve), real ablation h (solid curve), overall effective ablated depth $h_t=h_M+h$ (dotted curve). Calculated maximum surace temperature Ts (dash-dotted curve) saturates when real ablation starts.

stant) polymer density, and T_0 the ambient temperatue. The last (Arrhenius) term shall describe thermally activated first order bond breaking within the bulk materials: $1\text{-}n_b \xrightarrow{k(T)} n_b$.

Here, nb is the fraction of "broken" bonds per unit volume, and 1-nb the fraction of virgin bonds. $L \equiv \Delta H_b N_0$ is the enthalpy per unit volume required to break *all* bonds; $L > 0$ for endothermic reactions. ΔH_b is the enthalpy per bond and N_0 the total (initial number density of bonds. The equation of chemical kinetics is

$$\frac{\partial n_b}{\partial t} = v\frac{\partial n_b}{\partial z} + (1-n_b)k_0 \exp(-T_a/T) \qquad (4)$$

where k_0 is a preexponential factor. Equations (2) and (4) are coupled via the velocity v. We assume that the material is ablated when the number of broken bonds at the surface reaches a critical value.

The reaction may simultanously produce volatile species, which are trapped within the material and leave it only after the laser pulse.

Calculatins, performed with these equations lead to the results as they are presented in Figs. 1 and 2. The main features are : i) Ablation starts sharply with a front velocity that has its maximum value just after the onset. ii) The transition to the quasi-stationary ablation regime is faster than in the surface model. iii) Near threshold, the ablation depth h has a square-root dependenceon laser fluence, e.e., $h \propto (\phi - \phi_{th})^{1/2}$. The ablation velocity is very high even near ϕ_{th}. iv) With $\phi \approx \phi_{th}$ ablation starts well after the laser pulse. v) The depletion of species is species is responsible for the Arrhenius tail observed with fluences $\phi \leq \phi_{th}$. vi) Residual modification of material is maxiumu near the threshold. The model calculations applied to polymide (Kapton™ H) are in agreement with the experimental results, as demonstrated in Fig. 3.

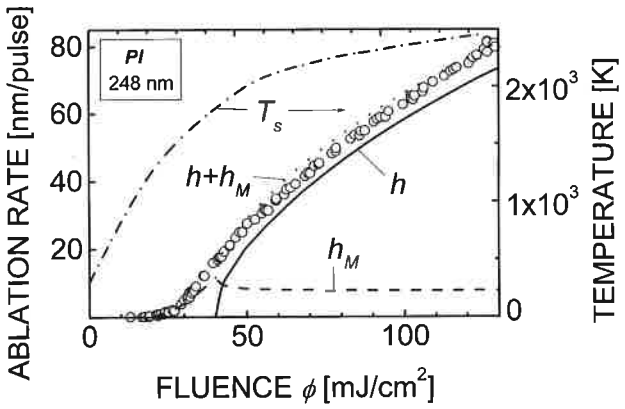

Figure 4. UV laser-induced surface topology hanges on PI. Left : AFM pictures (three-dimensional view). Right : cross section. (a) $\phi = \phi_{th}$=0.96, τ_l=5 μs ; and (b) $\phi = \phi_{th}$=1.01, τ_l=2.1μs.[3]

Single-pulse laser micropattering

We report on single-shot experiments using focused UV-Ar$^+$-laser radiation (wavelength $\lambda \approx 302$ nm, Gaussian beam profile, $w_o \approx 2.6$ μm). Here, the laser fluence, ϕ, is changed either via the laser beam intensity or via the pulse length, τ_l. The pulse lenght was controlled by a digitally driven acousto-optic modulator[12]. By these means, almost rectangular laser pulses with 140 ns $\leq \tau_l \leq$ 50 ms full width at half maximum were generated. The change in surface toplogy and the ablated depth have been studied by atomic force microscopy. Localized irradiation of polyimide with subthreshold fluences, result in the formatin of a hump as shown in Fig. 4(a). Hump formation has been tentatively explained by amorphization of the material and an additioanl volume increase related to

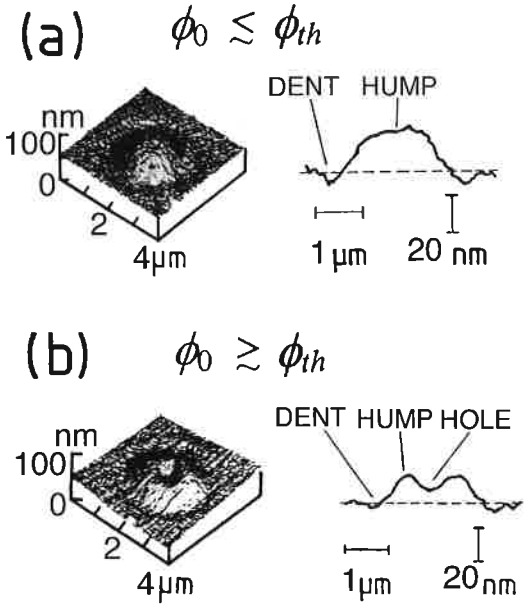

Figure 5. Dependence of threshold fluence for PI ablation on Ar$^+$-laser pulse duration ($\lambda \approx 302$ nm). Open symbols: reference data from XeCl-laser ablation (after Piglmayer *et al.*[3]).

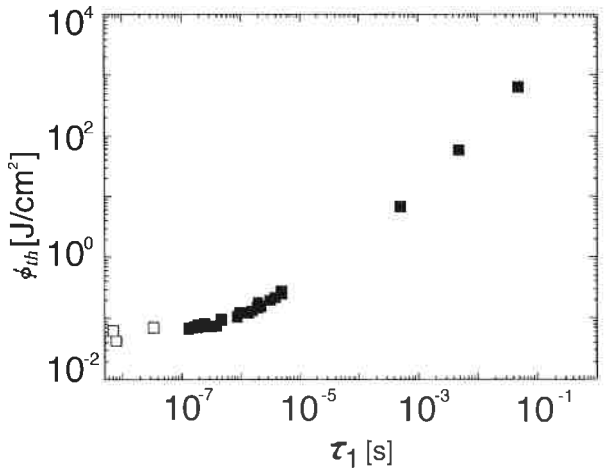

Figure 6. Schematic picture of an experimental setup employed in PLD.[1]

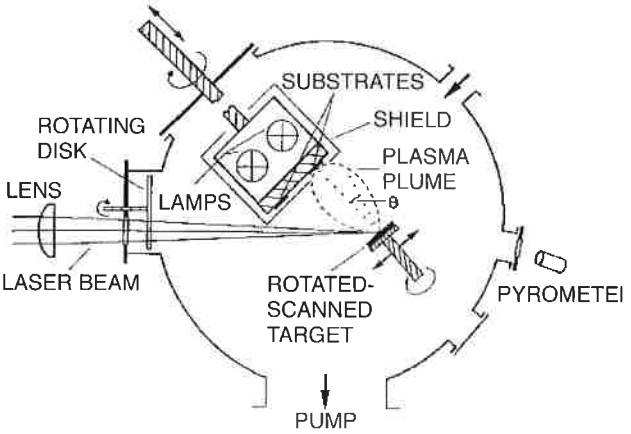

Figure 7. Optical polarization micrographs showing the surface morphology of KrF-laser deposited PTFE-Teflon films on Si substrates, λ = 248 nm, ϕ = 2.5J/cm^2, N_l = 2500 pulses, 2 Hz, T_s = 400°C and additional post-annealing at T_a = 550 (after Li *et al.*[4]).

polymer fragements trapped within the surface. This creates an internal pressure within the polymer. When real ablation starts, a dip apperas in the center of the hump, as shown in Fig. 4(b). Fig. 5 showns the threshold fluence, ϕ_{th}, as a function of τ_1. For comparison, also results of XeCl-excimer laser-ablation are included.[13,14,15] This dependence of ϕ_{th} on τ_1 is a strong indication that ablation with 302 nm cannot be based on a photochemical process.

Pulsed laser deposition of thin films

A typical setup employed for film deposition is schematically shown in Fig. 6. It essentially consists of a laser, a laser chamber, a target, and a substrate. The material ablated from the target is condensed on the substrate and froms a thin film. Ablation can take place in either a vacuum or a low pressure inert or reactive atmosphere. The targets mainly employed in PLD are ceramics and, in special cases, liquids. To a lower extent. targets in single crystalline, polycrystalline, powdery, or amorphous form are used as well. For uniform ablation, the target is rotated and scanned with respect to the laser beam.[16]

The good mechanical, thermal, and chemical stability of polytetrafluoroethylene (PTFE) together with its low surface adhesion, frictional resistance, and low dielectric constant, makes this material unique for numerous applications in mechanics, microelectronics, chemistry, medicine, and bioscience. For certain applications, it is desirable to fabricate PTFE in the form of thin films.

PTFE films were deposited by means of KrF-laser radiation from pressed powder targets (grain sizes between 6-9 μm).[4] The films are highly crystalline, as shown in the optical polarization micrograph of Fig. 7. The size of the spherulites can be enlarged to diameters up to 500 mm by postannealing at 550°C. The high crystallinity of the PLD-PTFE films is demonstrated in IR transmission spectra (Fig. 8),[4] where all bands related to amorphous PTFE are missing in the PLD films. PLD-PTFE films also show the characteristic first-order structural phase transitions from triclinic to hexagonal and pseudoxexagonal at 20 and 30°C, respectively. This is shown by dielectric characterization.[17]

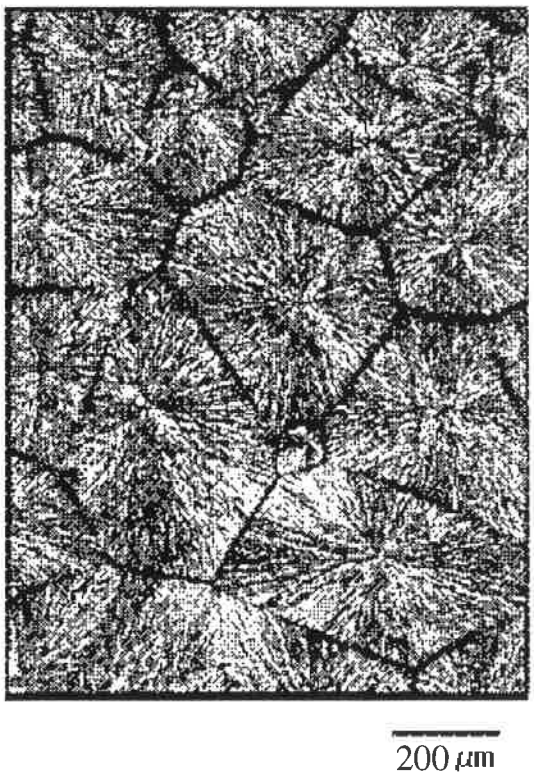

Figure 8. IR spectra for (a) a post-annealed film deposited from a pressed powder pellet at T_s = 355°C, T_a = 550°C, (b) a commercial PTFE foil (d = 25 μm) (after Li et al.[4]).

Particulates accompanying laser ablation

During film formation, PTFE grains are laser-transferred from the target to the substrate with subsequent melting and

crystallization. Interactions between particulates and the plasma plume seem to play an important role in the film formation process.[4]

We show that there are basically four types of particles generated under these conditions (pressed and sintered target, 1 atm air, presence of a visible plume implying plasma formation):

I. very small sub-micron particles
II 0.5 to 10 μm chains, consists of aggregated sub-micron particles
III. ~1 μm ejecta
IV. ~4-10 μm ejecta

For type I particles, the electrical charges appear to be of both signs. type II particles appear to be weakly charged or uncharged aggregates of type I particles (i.e., probably aggregates of both ±charges), which may explain their shapes and neutral character.

For type III particles, we are able to characterize their charge densities (assuming spherical shape)-we observe approximately equal numbers of ±charges with an average surface charge density of 10^{-5}-10^{-6} C/m^2.

For type IV particles we are able to show that they preferentially accumulate negative charge.

SEM micrographs of particulates of the various types are shown in Fig. 9. The electrical charge and particle diameter could be evaluated by the Millikan oil-drop experiment. The electrostatic surface charge density distribution of particles is depicted in Fig. 10.

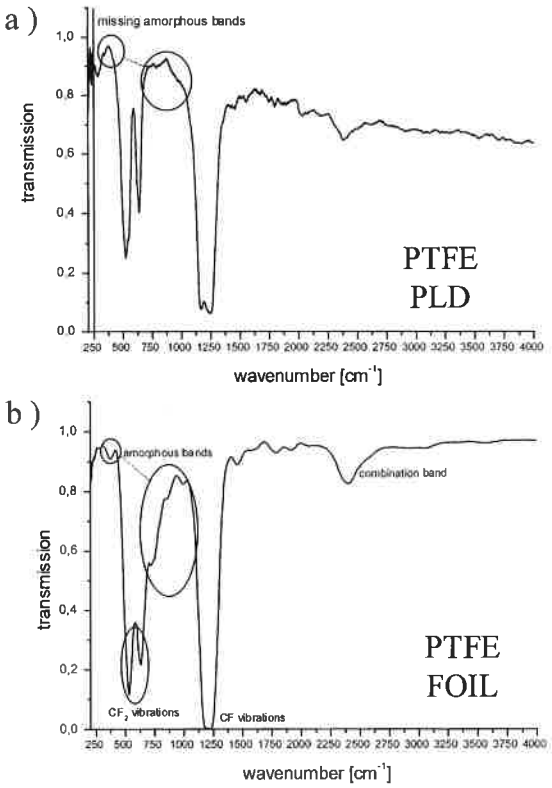

Figure 9. SEM micrographs of particulates ejected from the PTFE target due to laser irradiation collected on Si wafers (a-c) or on adhesive tape (d).[7]

The charge storage of PTFE particles is of considerable interest in developing charge storage devices. It is known that the charges are stored at layer near the film surface with a thickness of not more than some mm and possibly less than 1mm. Homogeneous volume charging can be achieved only if the samples are charged for a long time at very high voltages and/or at elevated temperatures. Our results show that the electrical charges for type III particles favor the surface over the bulk. Because the diameter of these particle is <2 μm, the fact that we see surface charging indicates that the thickness of the charged layer is probably in the sub-mm range.

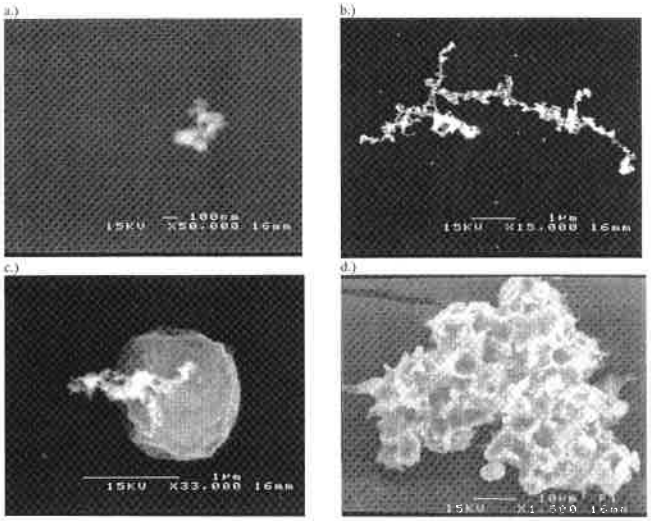

Figure 10. Histogram of the observed charge density assuming surface charge storage.[7]

Acknowledgements –This work was supported by the "Fonds zur Föderung der wissenschaftlichen Forschung under Contract P11981-PHY and Jubilämsfonds der Öterreichischen Nationalbank under Contract 7563. Partial support for this work was also provided by U.S. Department of Energy (Grants DE-FG03-98ER14864 and D-FG07-97ER62516).

REFERENCES

1. Bäuerle, D. (1996) Laser Processing and Chemistry. Springer Verlag, Heidelberg, Berlin.
2. Arnold, N., N. Bityurin (1999) Model for laser-induced thermal degradation and ablation of polymers. *Appl. Phys. A* **68**, 615-626.
3. Piglmayer, K., E. Arenholz, C. Ortwein, N. Arnold and D. Bäuerle (1998) Single-pulse ultraviolet laser-induced surface modification and ablation of polyimide. *Appl. Phys. Lett.* **73**, 847-849.
4. Li, S. T., E. Arenholz, J. Heitz and D. Bäuerle (1998) Pulsed-laser deposition of crystalline Teflon (PTFE) films. *Appl. Surf. Sci.* **125**, 17-22.

5. Schwödiauer, R., S. Bauer-Gogonea, S. Bauer, J. Heitz, E. Arenholz and D. Bäuerle (1998) Charge stability of pulsed-laser deposited polytetrafluoroethylene film electrets. *Appl. Phys. Lett.* **73**, 2941-2943.
6. Webb, R. L., J. T. Dickinson and G. J. Exarhos (1997) Characterization of particulates accompanying laser ablation of NaNo3. *Appl. Spec.* **51**, 707-717.
7. Heitz, J. and T. Dickinson (1999) Characterizatin of particulates accompanying laser ablation of pressed polytetrafluorethylene (PTFE) targets. *Appl. Phys. A* **68**, 515-524.
8. Küper, S., J. Brannon and K. Brannon (1993) Threshold behavior in polyimide photoablation: single-shot rate measurements and surface-temperature modeling. *Appl. Phys. A* **56**, 43-50.
9. Luk'yanchuk, B., N. Bityurin, M. Himmelbauer and N. Arnold (1997) UV-laser ablation of polyimide: from long to ultra-short laser pulses. *Nucl. Instrum. Meth. B* **122**, 347-355.
10. Bityurin, N., A. Malyshev, B. Luk'yanchuk, S. Anisimov and D. Bäuerle (1996) Photophysical mechanism of UV-laser action: the role of stress transients. *Proc. SPIE* **2802**, 103-112.
11. Frisoli, J. K., Y. Hefetz and T. F. Deutsch (1991) Time-resolved UV absorption of polyimied *Appl. Phys. B* **52**, 168.
12. Himmelbauer, M., E. Arenholz and D. Bäuerle (1996) Single-shot UV-laser ablation of polyimide with variable pulse lengths. *Appl. Phys. A* **63**, 87-90.
13. Andrew, J. E., P. E. Dyer, D. Forster and P. H. Key (1983) Direct etching of polymeric materials using a XeCl laser. *Appl. Phys. Lett.* **43**, 717-719.
14. Brannon, J. H., J. R. Lankard, A. I. Baise, F. Burns and J. Kaufman (1985) Excimer laser etching of polyimide. *Appl. Phys.* **58**, 2036-2043.
15. Dyer, P. E. and J. Sidhu (1985) Excimer laser ablation and thermal coupling efficiency to polymer films. J. *Appl. Phys.* **57**, 1420-1422.
16. Arnold, N. and D. Bäuerle (1999) Uniform target ablation in pulsed-laser deposition. *Appl. Phys. A* **68**, 363-367.
17. Schwödiauer, R., J. Heitz, E. Arenholz, S. Bauer-Gogonea, S. Baurer and W. Wirges (1999) Pulsed-Laser-Deposited and Plasma-Polymerized Polytetrafluoroethylene (PTFE)-Like Thin Films: A Comparative Study on PTFE-Specific Properties. *J. Polym. Sci. B: Polym. Phys.* in press.